BENGUET FOREST FIRE BURNED AREA & TAAL ASH EXTENT ESTIMATION USING SUPPORT VECTOR MACHINE & THRESHOLDING TECHNIQUES

Arlo Jayson Sabuito (1), Cara Patricia Canlas (1), Mark Jayson Felix (1) Gay Jane Perez (1)

[1] Institute of Environmental Science and Meteorology, University of the Philippines, Diliman, Quezon City, 1101, Metro Manila, Philippines

Email: acsabuito@stamina4space.upd.edu.ph, carac@stamina4space.upd.edu.ph, mjbfelix@stamina4space.upd.edu.ph, gpperez1@upd.edu.ph

KEY WORDS: Diwata-2, Support Vector Machine, Burned Area Index, Forest Fire, Ashfall Extent

ABSTRACT: Diwata-2 is the second Philippine microsatellite developed to provide Earth-observation data for disaster assessment and environmental monitoring. Since its launch in October 2018, the satellite has collected 25,811 images for various applications. In this study, the capability of Diwata-2 to monitor large-scale disasters is demonstrated through the identification of ash-stricken areas in the recent Taal Phreatic eruption and forest fire-affected areas of Benguet. Ashfall and burned area extent were classified from the Taal volcano eruption and Benguet forest fire, respectively. Diwata-2 images used were taken on January 6, 2020 and January 27, 2020 capturing the volcano's surrounding areas, and February 29, 2020 for areas in Benguet Province. The extent of both disasters' damages was delineated through index difference thresholding and Support Vector Machine (SVM) classification. For the index difference thresholding, Normalized Difference Vegetation Index (NDVI) and Burned Area Index (BAI) were used to identify ash stricken and burned areas, respectively. Similar methods were applied to Sentinel-2 for further evaluation using a higher resolution optical imagery. The ashfall extent measured from Diwata-2 was estimated at 20,359.64 ha and 55,669.24 ha for NDVI thresholding and SVM classification, respectively. The detected areas for both Diwata-2 and Sentinel-2 coincide with the major ash plume's general directions to the north and the subsequent ash plumes to the southwest direction of Taal volcano. In Benguet forest fire, the burned area extent was calculated to be around 2,714.59 ha using BAI thresholding. Identified fire occurrences for Diwata-2 and Sentinel-2 generally match with each other except for cloud-covered areas. Overall findings demonstrate the applicability of Diwata-2 satellite as a tool for large scale disaster monitoring and assessment in the Philippines. Future works include validation through field records and reports. The results underline the significance of remote sensing in disaster monitoring by providing spatial information to aid in emergency response, damage assessment, and future policymaking.

1. INTRODUCTION

Remote Sensing is inherently advantageous in disaster mitigation, monitoring, and response (Joyce et al., 2009a). It can be an ideal alternative for collecting and processing data for mapping, as it covers large spatial and temporal extents within a cost- and time-efficient framework (Koutsias, et al., 1999). Consequently, increasing demands for remotely sense data geared investments towards research and development of smaller and cheaper satellites that can manage the same job (Xue, et al., 2008).

Diwata-2 is a 50-kg earth observation Philippine microsatellite launched in October 2018. The microsatellite onboards five payloads, namely, Spaceborne Multispectral Imager (SMI) with Liquid Crystal Tunable Filter (LCTF), High Precision Telescope (HPT), Middle Field Camera

(MFC), Wide Field Camera (WFC), and Enhance Resolution Camera (ERC). In addition to these payloads, Diwata-2 also carries deployable solar array panels, and Amateur Radio Unit (ARU). These payload and additional features support one of the satellite's key missions and objectives, post disaster assessment.

Last January 12, 2020, a phreatic eruption of Taal Volcano was reported in the province of Batangas, Philippines. The eruption resulted in ash fall observed in the adjacent regions of Metro Manila, and CALABARZON. The coverage of the ashfall reached up to Central Luzon, and Ilocos region brought by the prevailing winds at the time of the eruption. The heavy ashfall has affected several provinces' economies, substantially the agricultural, livestock, and fisheries sector reaching P 3.06 billion damage and loss (DA Communications Group, 2020). The following month, recorded incidents of forest fire in the province of Benguet; alarmingly affecting established tree plantation of the National Greening Program and natural pine forests was reported (Ongpin, 2020). Containing the spread of fire had been difficult due to the province's topography consisting of mountain terrain, steep slopes, and inaccessible roads. According to the Philippine Information Agency Benguet, 10 out of 13 towns were affected in the province with 12 significant forest fires (Philippine Information Agency, 2020).

To aid in the post-disaster response, Diwata-2 was tasked to acquire images relating to these events. These acquisitions were used to identify the areas affected by the ashfall in Batangas, and burned vegetation cover due to the forest fire in Benguet. Remote sensing techniques have been used for post disaster situations. Various approaches in change detection exist, namely, image thresholding, and image classification. The first method is value thresholding relevant indices to isolate the pixels corresponding to affected areas. Several indices can be used as an indicator of change characterized by the incident. Normalized Difference Vegetation Index (NDVI), and burn indices are some of the established measures in remote sensing for environmental monitoring, and change detection (Escuin, S., et al., 2008 and Chuvieco, 1999). The second method is supervised classification utilizing support vector machines (SVM). This classifier has achieved a higher level of accuracy compared to generally accepted methods of classification in remote sensing applications such as using the Maximum Likelihood Classifier (MLC). This machine learning method allows small training samples, and still produces a sufficient change detection result in several studies (Oommen, et al., 2008 and Wieland, et al., 2016). This operates by setting a hyper-plane which will optimally separate classes through regularization parameters and gamma. This addresses the curse of dimensionality wherein data is mapped into feature space; and utilizes kernel function which projects the data in a suitable feature space. SVM exhibits good generalization of data and discriminant in changes on both single and multitemporal feature space (Camps-Valls, et al., 2009).

Post disaster assessment through satellite image classification is one way to utilize space technology in aiding disaster response. Mapping the extent of damage is significant information for resource management and monitoring. Assessment of affected areas, and casualties can be translated to direct economic losses in assistance to disaster risk management and decision making.

The utility of Diwata-2 is the metric by which the compact space mission will be measured. Following this, this paper aims to use the images captured by the microsatellite to create post disaster assessment of the said events. The extent of affected areas will be determined and quantified through established remote sensing techniques, image thresholding, and support vector machine classification.

2. METHODOLOGY

2.1 - Study Sites

Diwata-2 acquisitions for the before and after the Taal eruption are dated January 6 & 27, 2020 respectively. The Taal image stretches from the provinces of Cavite, Laguna, and Batangas. The volcano sits in Batangas province, distinctively located within a lake within an island shown in Figure 1. Taal Volcano is a compound volcano, secondly active volcano in the Philippines (Pfeiffer, 2020). Its eruptive history has caused casualties, and destruction of properties in its vicinity.

For the mapping of forest fire affected areas in Benguet, Diwata-2 was able to capture the area on February 29, 2020. Benguet is a landlocked province located in the Cordillera Administrative Region (CAR), Luzon. The province predominantly mountainous occupying the part of the Cordillera Mountain range, and the highest mountain in Luzon, Mount Pulag. Almost 66 - 80% of the area are primarily forests and shrublands. The setting is also rich with various landforms devising the province's economic activities such as tourism, mining, and agriculture specifically, rice terraces, root crops, swidden farming, livestock, and hunting (Chua-Barcelo, 2014).

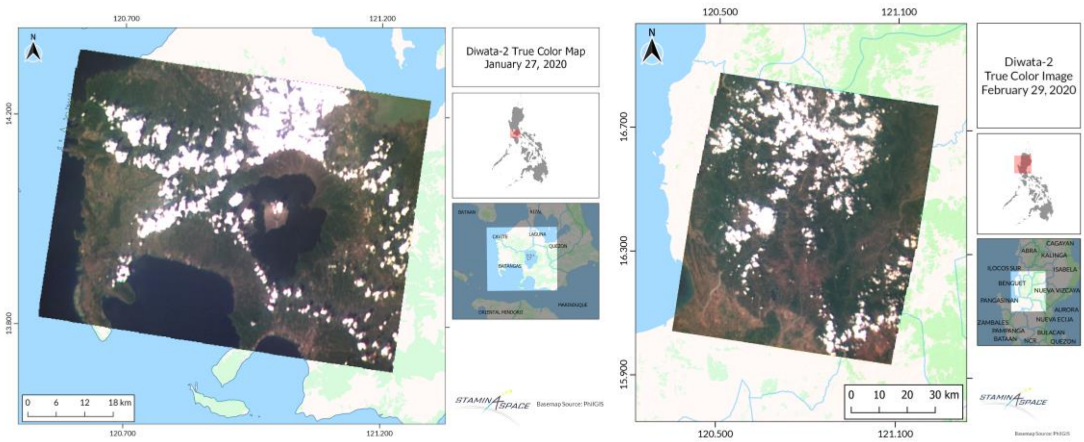

Figure 1. Diwata-2 acquisitions of Taal area (left), and Benguet Province (right).

2.2 - Satellites

The images captured by the SMI payload onboarding Diwata-2 were primarily used in this study. In addition to the microsatellite, Sentinel-2 was used to complement the result. The Copernicus Sentinel-2 mission is composed of a pair of polar orbiting satellites, Sentinel-2A & 2B which provides high resolution Earth observation data. Each satellite carries a Multi-spectral Instrument (MSI) utilized for land monitoring, emergency management, security, and climate change. Satellite specifications for Diwata-2, and Sentinel-2 are shown in the table 1.

Table 1. Satellite Resolution.

	Spectral Resolution	Temporal Resolution	Spatial Resolution
Diwata-2 SMI	400 - 1000 nm	11 days	127 m
Sentinel 2 MSI	13 bands	5 days	10 m, 20 m, 60 m

2.3 - Workflow

General workflow for Diwata-2 images is illustrated below. Different approaches were carried out for each disaster such as index option, training bands, and thematic classes for training data.

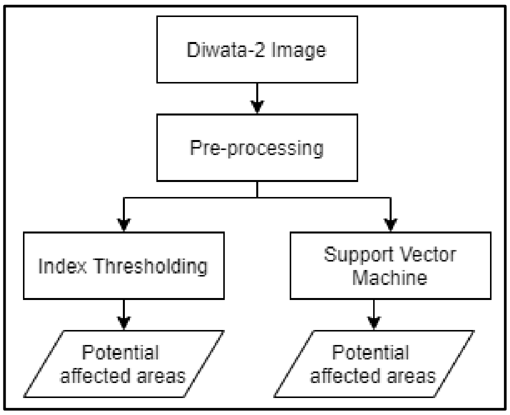

Figure 2. Post disaster assessment using Diwata-2 image general workflow.

Diwata-2 preprocessing involves mosaicking, cloud masking, and atmospheric correction of Top-of-Atmosphere (TOA) Reflectance products. Mosaicking was done using a Python script while cloud masking and atmospheric correction were processed using ENVI. Quick Atmospheric Correction (QuAC) was used on the Near-infrared, red, green, blue bands of the Diwata images to acquire surface reflectance products for further processing.

2.4 - Index Thresholding

Indices were used to detect ash extent, and burned area for Taal eruption, and Benguet forest fire, respectively. Normalized Difference Vegetation Index (NDVI) was used for the ashfall event since the affected areas are mostly covered in vegetation and has been an effective parameter in identifying vegetation changes. NDVI equation is expressed in Eq (1)

$$\boldsymbol{NDVI} = \frac{\boldsymbol{NIR} - \boldsymbol{Red}}{\boldsymbol{NIR} + \boldsymbol{Red}} \tag{1}$$

The difference of derived NDVI for pre and post eruption was calculated. This was to determine pixels with abrupt change in value and were flagged as affected areas. Before the same method was done with Sentinel-2 surface reflectance products, a quality mosaic of historical images from October 2019 up to January 10, 2020 was made using Google Earth Engine to minimize cloud contamination. Optimal threshold values for the difference map was determined by a priori knowledge of the affected areas based on volcanic activity, wind direction and new reports.

Burn Area Index (BAI) was used to map burned areas in Benguet. The index uses convergence points of the red and NIR bands, defined as 0.1 and 0.06 (Chuvieco, 1999), surface reflectance of red band, ρ_{red}, and surface reflectance of NIR band, ρ_{NIR}. This highlight burned areas in the red and NIR spectrum. Distinct values between burned, and other features were used to identify the affected areas. BAI equation is expressed in Eq (2)

$$BAI = \frac{1}{((0.1 - \rho_{red})^2 + (0.06 - \rho_{NIR})^2)} \quad (2)$$

2.5 - Support Vector Machine Classification

The Support Vector Machine algorithm provides an effective way for supervised classification of remotely sensed data. This machine learning technique digests training sets of data representative of themes that are of interest to the user. In this study, Radial Basis Function (RBF) kernel function is used, commonly utilized for remote sensing applications, and shows best results.

The classifier creates a land cover map with thematic information of interest, in this case, ashfall and burned area. Image composite of VIS-NIR and index was used for training bands. BAI and NDVI were used for Benguet acquisition, and Taal acquisition, respectively. Image composite of pre and post disaster images were also used for Taal ash extent estimation before training the classifier to account for the change due to ash covering the land cover.

Training data were created categorizing general classes of vegetation (e.g. dense, and sparse vegetation), non-vegetation (e.g. built-up, bare), water (e.g. turbid water, inland water, optically deep water), ash, and burned area. Subclasses were also created specific for each mission. Homogenous pixels of these classes were selected to lessen variation from mixed pixels.

3. RESULTS AND DISCUSSION

3.1 - Index Thresholding Results

NDVI difference of the pre and post images taken around the volcano. High- and low-end values signify significant temporal change. The low-end values mostly capture the shift in spectral values of vegetation cover due to ash. NDVI values for this class are distinguishable with ash and mostly cover the surrounding regions of the volcano; apt for identifying land cover changes.

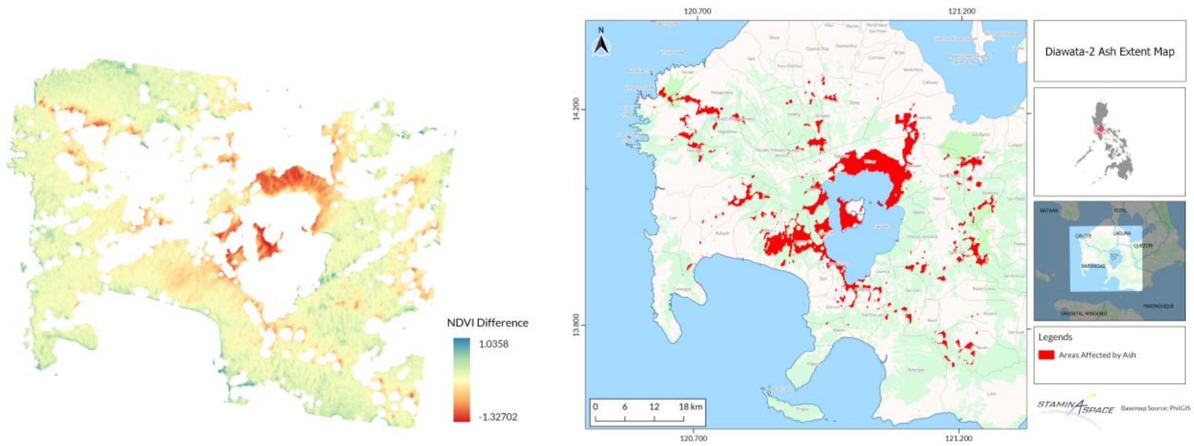

Figure 3. NDVI Difference result (left), and ashfall extent using thresholding (right) of Taal study site.

Figure 3 shows the result of index difference thresholding. Estimates from the method reveal 20,359.64 ha of ash extent in portions of CALABARZON and NCR. False detection often manifests from cloud shadows and hill shade. Cloud cover to the north of the lake limited the detection where it is supposedly most affected. Mildly affected areas in the southwest were also detected to a certain degree.

Prior to Diwata-2 acquisition, Benguet province has already experienced forest fires as early as the beginning of February. Burned areas are displaced throughout the province's land cover. A visual analysis of the index result shows distinction between burned and unaffected areas. High index values are observed on affected areas shown in yellow to blue colors of Figure 4. With the addition of the index, more instances of burned areas were observed which were barely noticeable in the RGB composite. However, classified burned areas mixed up with classes with similar values like thin cloud edges, bare soil, and casted shadows. Deliberate selection of convergence point between the affected areas was carried out to identify high confidence burned areas. These were delineated through image thresholding leaving burned areas shown in Figure 4. Extent of the incident was computed covering 2,714.12 ha of burned areas in Benguet Province.

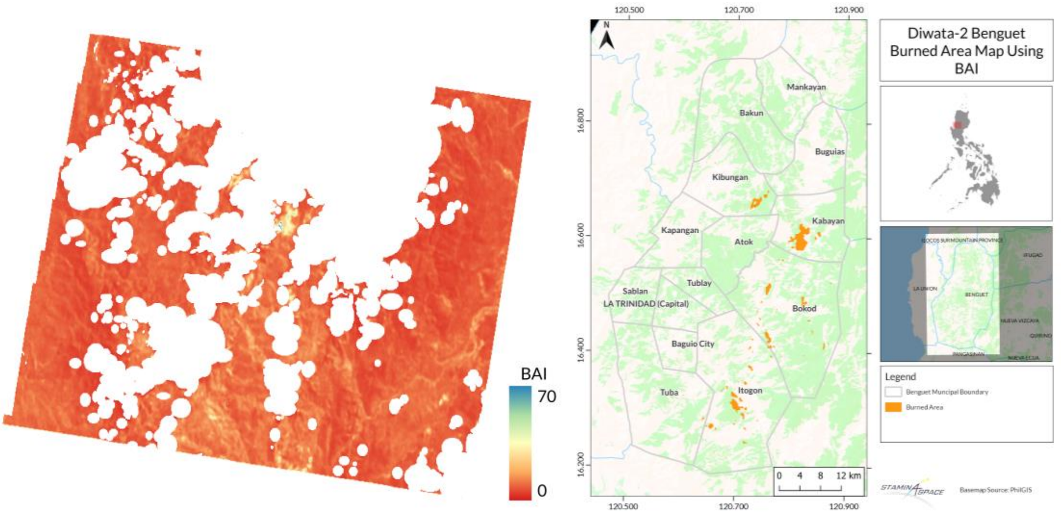

Figure 4. Burn Area Index result (left), and burned area using thresholding (right) of Benguet forest fires.

3. 2 - Support Vector Machine Results

Through the SVM classification workflow, affected areas for the Taal eruption were estimated to be around 55,669.24 ha. Figure 5 shows the detected class for the ash-stricken areas. Similar clusters from the index threshold in the north and southwest regions of the volcano were detected. Additionally, shadows casted by clouds persist as the main cause of false detection. This method however shows greater detection rate for mildly affected areas as seen in the south western region.

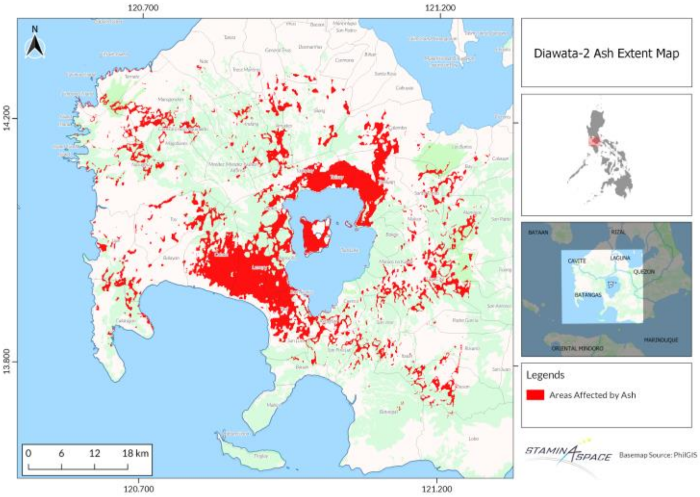

Figure 5. Diwata-2 ashfall extent result using SVM classification.

Burned areas detected through SVM classifier have a total computed total area of 5,182.25 ha. With the addition of BAI as training data, results show improved classification detecting cloud edges, cloud shadow, and distinction between them vs. burned area. However, overestimation of result is still observed contributed by the elevated surface's shadow. Similar spectral signatures from the hill shades resulted to be categorized to burned area class inducing false detection.

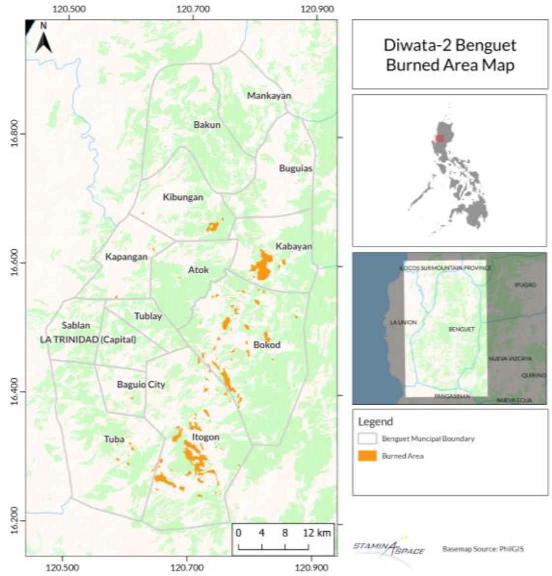

Figure 6. Diwata-2 burned area results using SVM classification.

3.3 - Result Validation

Other than news reports of majorly affected areas in the vicinity of the volcano and minor ashfall further up north, no actual ground validations were carried out and recorded. Furthermore, ash can easily be washed away in a short period of time due to wind and precipitation. Consequently, to complement the detection done using Diwata-2, we turn to the results from Sentinel-2, an established earth observation mission, using the same methods. Figures 7 show the detection of ashfall extent by thresholding and SVM, respectively.

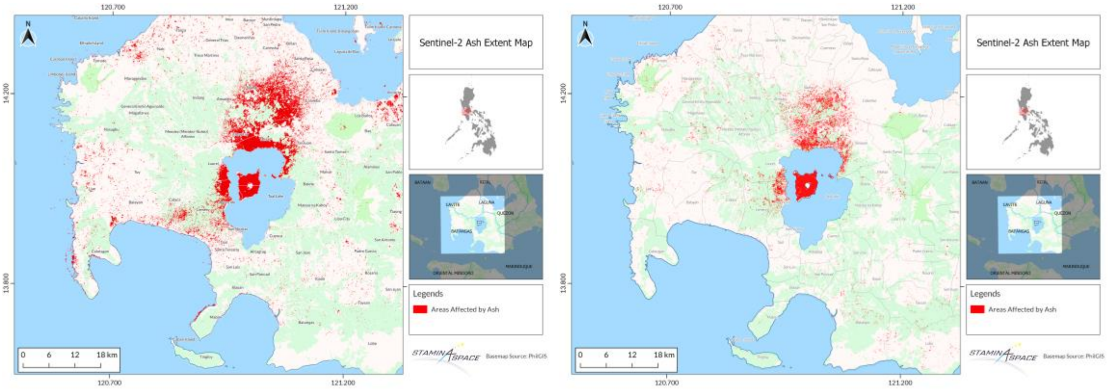

Figure 7. Sentinel-2 ashfall extent results from index thresholding (left), and SVM classification (right).

Results show general consistency in direction of detected areas with the Diwata-2 findings. Similarly, thresholding shows less detection compared to SVM. Detection of mildly affected areas for both methods appears to be less prominent compared to Diwata-2. This may be caused by spectral mixing due to coarser spatial resolution of the latter causing generalization in classification. More areas to the north are detected due to better weather conditions for remote sensing.

SVM classification was also applied to Sentinel-2 MSI data for burned area detection shown in Figure 7. Results show detected burned areas comparable to Diwata-2 findings. Affected areas from both satellites are present in the towns of Kabayan, Kibungan, Bokod, and Itogon. Considering the Sentinel-2 image date, subsequent forest fires may have spread, Diwata-2 burned area results show additional towns affected.

Complementing the index threshold, and classification results from Diwata-2 and Sentinel-2, data from Fire Information for Resource Management System (FIRMS) has monitored the fire occurrence of the province using MODIS brightness temperature channels 21/22 for active fire pixel measurement shown in Figure 8. In addition to this, a confidence band is used intended to help users gauge the quality of individual active fire pixels. Diwata-2 identified burned areas coincides with the FIRMS dataset at > 50% confidence, in towns of Kibungan, Kabayan, and Bokod. With the dataset's spatial resolution at 1 km, this has limited registrations of small-scale fire occurrences as opposed to Diwata-2 and Sentinel-2 results.

On the other hand, local government units in Benguet have ground reports of the occuring forest fire, recording fires except the towns of Mankayan, Kapangan, and Sablan (Philippine Information Agency, 2020).

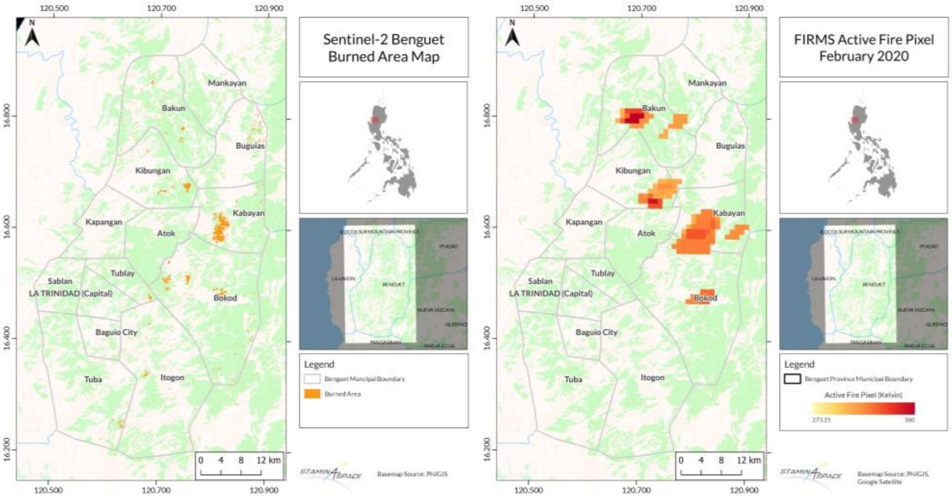

Figure 8. Sentinel-2 burned area map using SVM (left), and FIRMS active fire pixel data of February 2020 (right).

4. CONCLUSION

In summary, Diwata-2 SMI was able to demonstrate post disaster assessment on the incidents of Taal eruption, and Benguet forest fires. Common remote sensing techniques such as image thresholding, and support vector machine classification were able to identify affected areas.

The ashfall extent measured from Diwata-2 was estimated 20,359.64 ha and 55,669.24 ha for NDVI thresholding and SVM classification, respectively. Diwata-2 measured 2,714.59 ha, and 5,182.25 ha of burned areas in Benguet using BAI thresholding, and SVM classification, respectively.

The mapped affected areas from Diwata-2 images coincided with satellite images from Sentinel-2 for both incidents. Additional data from Sentinel-2, FIRMS, and grounds reports provides complementary, and validity of Diwata-2 results for the forest fire assessment. False detections have generally been observed from feature shadows in the two cases.

Mapping the extent of damage is significant information for resource management and monitoring. Assessment of affected areas, and casualties can be translated to direct economic losses in assistance to disaster risk management and decision making. Testing the capability of small-scale space missions such as Diwata-2 to perform these crucial tasks is an important step towards cost-effective earth observation especially in developing countries such as the Philippines.

References

Camps-Valls, G & Bruzzone, L., 2009. Kernel Methods for Remote Sensing Data Analysis. (1st ed.) Wiley.

Chua-Barcelo, RT., 2014. Ethno-botanical survey of edible wild fruits in Benguet, Cordillera administrative region, the Philippines Asian Pacific Journal of Tropical Biomedicine, 4 (1), pp. S525-S538

Chuvieco, E., 1999. Remote Sensing of Large Wild res in the European MediterraneanBasin (Berlin: Springer)

DA Communications Group, 2020. Agri damage from Taal reaches 3B. Retrieved June 27, 2020, from https://www.da.gov.ph/agri-damage-from-taal-eruption-reaches-php3b/

Escuin, S., Navarro, R., & Fernández, P., 2008. Fire severity assessment by using NBR and NDVI derived from LANDSAT TM/ETM images. International Journal of Remote Sensing, 29(4), 1053–1073.

Joyce, K.E., Wright, K.C., Samsonov, S.V., & Ambrosia, V.G., 2009a. Remote sensing and the disaster management cycle.

Koutsias, N., M. Karteris, A. Fernandez-Palacios, C. Navarro, J. Jurado, R. Navarro, and A. Lobo. 1999. “Burned Land Mapping at Local Scale.” In Remote Sensing of Large Wildfires in the European Mediterranean Basin, edited by E. Chuvieco, 157–187. Heidelberg: Springer-Verlag.

Oommen, T., Misra, D., Twarakavi, N. K. C., Prakash, A., Sahoo, B., & Bandopadhyay, S., 2008. An Objective Analysis of Support Vector Machine Based Classification for Remote Sensing. Mathematical Geosciences, 40(4), 409–424.

Ongpin, Ma. I., 2020. Alarming Benguet forest fires. Retrieved June 25, 2020, from https://www.da.gov.ph/agri-damage-from-taal-eruption-reaches-php3b/

Pfeiffer, T. (2020). Taal volcano. Retrieved from https://www.volcanodiscovery.com/taal.html

Philippine Information Agency, 2020. Community, barangay officials called to help to prevent forest fires. Retrieved June 29, 2020, from https://www.philippinesnews.net/news/264229493/community-barangay-officials-called-to-help- prevent-forest-fires

#ResilienceCaravan, 2020. Retrieved June 29, 2020, from https://www.facebook.com/PIABenguetInfocen/posts/3293543510871287

Wieland, M., Liu, W., & Yamazaki, F., 2016. Learning Change from Synthetic Aperture Radar Images: Performance Evaluation of a Support Vector Machine to Detect Earthquake and Tsunami-Induced Changes. Remote Sensing, 8(10), 792.

Xue, Y., Li, Y., Guang, J., Zhang, X., & Guo, J., 2008. Small satellite remote sensing and applications – history, current and future. International Journal of Remote Sensing, 29(15), 4339–4372. doi:10.1080/01431160801914945